Published in *Microporous and Mesoporous Materials, vol. 121, pp. 129-137 (2009)*
http://dx.doi.org/10.1016/j.micromeso.2009.01.034

Tailoring the acid strength of microporous silicoaluminophosphates through the use of mixtures of templates: control of the silicon incorporation mechanism

Luis Gómez-Hortigüela, Carlos Márquez-Álvarez, Marisol Grande-Casas, Raquel García and Joaquín Pérez-Pariente*

Instituto de Catálisis y Petroleoquímica. CSIC. C/ Marie Curie 2. 28049 Cantoblanco. Madrid. Spain.

* Email: lhortiguela@icp.csic.es

ABSTRACT. SAPO-5 samples have been synthesized with triethylamine (TEA), benzylpyrrolidine (BP) and mixtures of them as structure directing agents (SDAs). It has been observed that in the as-synthesised materials the concentration of SDAs (molecules per unit cell) and the Si content are similar. According to the different molecular size of both SDAs, the samples exhibit higher organic weight and lower water content as the molar fraction of BP in the synthesis gel increases. These differences in selectivity for organic/water incorporation influences the mechanism of Si substitution in the AlPO lattice: the higher organic content obtained at higher BP/TEA ratio leads to the formation of large Si islands, while the higher water content of the sample obtained with TEA enhances the formation of isolated $Si(OAl)_4$ environments.

Interestingly, it has been found that these two opposite trends can be tailored to a certain point by using mixtures of both SDAs, TEA and BP, in the required ratio. The catalytic activity of the samples has been tested in the isomerisation of m-xylene. It has been observed a higher activity of samples obtained with BP as the main SDA, thus evidencing the better performance of large Si islands in this reaction.

KEYWORDS: silicoaluminophosphate, structure directing agents, water, catalytic activity, microporous structure, acid strength, silicon incorporation mechanism.

Introduction

Since the discovery of microporous aluminophosphates (AlPO) by Wilson *et al.* in 1982 [1], the synthesis of these materials has been widely studied, yielding a diversity of structural types comparable to that of the previously known aluminosilicate-based zeolites [2]. Known microporous AlPO structures include polymorphs that are common to both SiO_2 and AlPO compositions, but also structures that have no zeolitic counterpart. In these AlPO materials, there is a strict alternation of Al^{3+} and P^{5+} ions; nevertheless, both ions can be isomorphically replaced by heteroatoms through different substitution mechanisms. The most common one is the replacement of Al by a divalent metal that gives a negative charge to the framework, which is usually charge-balanced by the organic cationic molecules that act as structure directing agents. However, Si^{4+} can also be incorporated in AlPO networks, giving place to acid catalysts with very interesting properties. Silicoaluminophosphates (SAPOs) have attracted considerable attention due to potential industrial applications; SAPOs have been tested for several acid-catalysed reactions such as isomerisation of xylenes [3-5], transalkylation [6],

isomerisation of 1-pentene [7], isopropylation of benzene [8], methanol-to-hydrocarbons reaction [9] and oligomerization of propylene [10].

The incorporation of silicon in AlPO frameworks is a special case where two different substitution mechanisms can simultaneously occur [11,12]. Silicon (Si^{4+}) can be incorporated via SM2 (Substitution Mechanism 2), that consists in the substitution of a single phosphorus ion (P^{5+}) for one Si (Si^{4+}), giving a negative charge per Si in the framework that is usually balanced by the positive charge of the organic molecules occluded within the microporous structure. This substitution mechanism gives an environment of Si surrounded by 4 Al atoms (in the second coordination shell, $Si(OAl)_4$). In the other mechanism (SM3), the incorporation of Si occurs via a simultaneous substitution of a pair of adjacent Al^{3+} and P^{5+} ions by two Si^{4+} ions, giving no net charge. Due to the instability of Si-O-P bonds, the latter mechanism is always accompanied by a certain extent of SM2 in order to prevent the formation of those unstable bonds, thus giving rise to silica domains (commonly referred to as Si islands) in the AlPO network. The simultaneous occurrence of both mechanisms results in the presence of different Si environments ($Si(OAl)_n(OSi)_{4-n}$, where n varies between 1 and 3). These environments are located at the border of the Si island, at the interface between the islands and the Al-O-P framework. Depending on the ratio of SM3 to SM2 substitutions, the size and concentration of the Si islands will be different.

In SAPO materials, Brønsted acidity rises when the negative charge of the framework (induced by the incorporation of Si through the SM2) is compensated by H^+, usually after calcination or ionic exchange of the cationic organic molecules. In the Si islands, the acidity is generated at the border, associated to the presence of $Si(OAl)_n(OSi)_{4-n}$ environments. It has been observed that the strength of the acid sites generated at the border of the Si islands is usually higher than that of the acid sites created by the

isolated Si atoms ($Si(OAl)_4$), and increases as the value of n in those environments decreases [13]. In addition, it is generally accepted that the strength of the acid sites generated at the border of the Si islands increases with the island size. In summary, a higher number of acid sites are generated through SM2, while SM2+SM3 yields less but stronger acid sites. Therefore, controlling the incorporation of Si through the different mechanisms would enable a control of the acidity of the materials, what would be very desirable for designing new and efficient catalysts for selected reactions. Following this aim, there have been many works on potential ways of controlling the Si incorporation into AlPO networks, especially by modifying the synthesis parameters [14,15]. An important improvement in the catalytic activity of SAPO materials was provided by the use of non-aqueous solvents (hexanol) and surfactants in the synthesis gels, which produced higher dispersion of Si in the crystals and smaller particles [4]. In our case, we aimed to control the Si incorporation via the rational use of the organic structure directing agents.

The synthesis of microporous materials involves the use of hydrothermal methods, where the source of the inorganic ions, water and, generally, an organic molecule, are heated in an autoclave for a certain period of time. The inclusion of organic molecules is usually required to direct the crystallization of a certain microporous structure, and so they are called structure directing agents (SDAs). The role of these organic molecules has been traditionally described as a “template effect” [16] to indicate that the organic molecules organize the inorganic tetrahedral units into a particular topology around themselves during the nucleation process, providing the initial building blocks from which crystallization of the microporous structures will take place. Nevertheless, the action of the SDA molecules is not limited to their role in structure-directing the crystallization of the microporous structure, but they can also influence the substitution

mechanisms by which Si is incorporated in the AlPO frameworks. Barthomeuf and coworkers studied the role of the SDA molecules in directing the Si incorporation in the network of SAPO-34 [17]. They observed that the occurrence of the different mechanisms whereby Si is incorporated depends on the organic SDA employed in the synthesis. It was concluded that Si substitution is governed by the number and charge of the SDA molecules that can be packed within the structure in order to charge-balance the negative charge generated by the inclusion of Si through SM2. A recent work has also evidenced the influence of the organic SDA employed in the synthesis over the distribution of Si in the AEL structure [18], leading to SAPO-11 materials with different catalytic activities. These works suggest that, at least in principle, the Si incorporation, and thus the acid strength of SAPO materials, could be controlled by a rational use of the organic molecules that structure-direct the crystallization of the microporous material. In a recent work we studied the structure directing effect in the presence of water of three different SDA molecules, triethylamine (TEA), benzylpyrrolidine (BP) and (*S*)-(-)-*N*-benzylpyrrolidine-2-methanol (BPM), in the synthesis of AlPO-5 (AFI type structure) [19]; this is a large-pore microporous structure composed of one-dimensional 12 membered-ring (MR) channels with a diameter of 7.3 Å [2]. In that work we observed an important and complementary role that water molecules play in the structure direction of the microporous structure. Interestingly, we observed a higher water occlusion within the AFI structure when the synthesis was performed with TEA as the SDA, while the use of the aromatic molecules (BP and BPM) led to a lower water occlusion, specially in the material obtained with BPM. Such a difference in the water/organic occlusion would in principle lead to a notable distinction in the hydrophilic/hydrophobic character of the channels of the microporous material. In last term, this could eventually lead to a different incorporation of Si in the AFI structure,

since the incorporation of Si as Si islands would impart a more hydrophobic character to the network, while the predominance of SM2 mechanism would result in more hydrophilic materials. Based upon these grounds, we wondered whether the use of these different SDAs, and thus the different hydrophilicity of the resulting AFI materials, could provide a control over the Si incorporation, and would thus afford a fine-tuning of the acid strength of the obtained catalysts. Due to the high cost associated to the use of BPM as SDA, and thus the low interest of this molecule to be used in potential applications, only TEA and BP molecules will be studied in this work. Not only samples obtained with pure TEA and pure BP will be prepared, but also materials in which mixtures of both SDAs are used, in order to determine whether the features promoted by the use of the different SDAs can be modulated in this way.

Experimental details

Triethylamine (TEA, 99 %) was purchased from Sigma-Aldrich. The synthesis of benzylpyrrolidine (BP) was carried out by reacting pyrrolidine (Sigma-Aldrich, 99 %) with benzyl chloride (Sigma-Aldrich, 99 %) in ethanol (90 ºC, 24 h) in the presence of potassium carbonate (Sigma-Aldrich, 99 %). The tertiary amine was extracted with chloroform and purified by vacuum distillation. The purity of the amine and its chemical formula was assessed by thin layer chromatography (hexane/ethyl acetate as solvent) and CHN chemical analysis (Perkin-Elmer 2400 CHN analyzer).

The synthesis gels were prepared with the following molar composition: *x* TEA : *y* BP : 1.0 P_2O_5 : 1.0 Al_2O_3 : 0.5 SiO_2 : 40 H_2O, keeping a constant total SDA (TEA + BP) concentration of 1.5 (x + y = 1.5). 1.5, 1.0, 0.5 and 0 values for 'x' (0, 0.5, 1.0 and 1.5 for 'y', respectively) were studied. The gels were prepared by adding the aluminium source, pseudoboehmite (Catapal Pural SB, 75.3% wt Al_2O_3), to a solution of

phosphoric acid (Riedel-de Haen, 85% wt) and water and stirred for 1h in a closed recipient (having a hole for the stirrer). The corresponding necessary amount of organic was then added (taking into account the addition of organic for the hydrolysis of TEOS, see below), and the stirring maintained for 2 h. The silicon source (tetraethylorthosilicate, TEOS, Merck, 99 %) was previously hydrolysed in the presence of water and the organic molecule (40 % of the necessary amounts) in a different vessel and the solution stirred until all the ethanol coming up from the hydrolysis of TEOS was evaporated; then it was added to the synthesis gels in the last step (after the addition of the remaining organic), and stirred for two more hours. The pH of the resulting gels was in a range between 3.5 and 4.1. The gels were introduced into 60 ml teflon lined stainless steel autoclaves and heated statically at 170 ºC for 16 hours. The resulting solids were separated by filtration, washed with ethanol and water and dried at 60 ºC overnight.

Calcination of the samples was carried out by passing an oxygen stream enriched in ozone (3-4 %) at 200 ºC for 24 hours. Complete removal of the organic molecule was assessed by TGA.

The crystallization of the AFI structure as a pure phase was assessed by X-Ray Diffraction (Seifert XRD 3000P diffractometer, CuKα radiation). Nitrogen adsorption-desorption isotherms were measured at -193 °C using a Micromeritics ASAP 2010 volumetric apparatus. All the samples exhibited isotherms characteristic of microporous solids, with a micropore volume (t-plot method, using the Halsey equation) of ca. 0.09 cm^3/g, total pore volume in the range 0.17-0.23 cm^3/g, BET surface area in the range 330-350 m^2/g, and external surface area ranging from 90 to 120 cm^3/g.

The organic content of the samples was studied by chemical CHN analysis (Perkin-Elmer 2400 CHN analyzer) and thermogravimetric analysis (TGA) (carried out in air,

with a Perkin-Elmer TGA7 instrument, ~5 mg of sample, heating rate = 20º/min). In order to be able to quantitatively compare the amount of water occluded in the materials, the samples were kept for 24 hours under an atmosphere with a controlled humidity of *ca.* 31-32 % (given by a saturated solution of $MgCl_2 \cdot 6H_2O$ kept at room temperature) prior to the thermal analyses. On-line thermogravimetric-mass spectrometry analyses (TG-MS) of the gases evolved from the sample were carried out on the Perkin-Elmer TGA 7 thermobalance coupled to a Fisons MD-800 quadrupolar mass spectrometer through a transfer line heated at 150 °C. The TGA range was from 30 to 900 °C at 20°/min under a continous flow of He (100 cm^3/min). A Perkin-Elmer transfer line, specially designed to avoid mass discrimination and connected to a vacuum pump in order to optimize the amount of gas sample transferred from the TG to the MS, carries on the evolved gases to the spectrometer. The ionization of the sample was done by electronic impact, using an ionization potential of 70 eV, with a 6 scan/min frequency and an atomic mass range of 2-200 a.m.u. Note that in this case, TGAs were carried out in a helium atmosphere (in contrast to normal TGA performed in air). Mass spectra of the organic species desorbed from single SDA-containing SAPO-5 samples (recorded at temperatures where the main desorption came from the organic molecules) indicated that the m/z values of the most representative fragment for TEA was 86 (corresponding to the $(CH_3CH_2)_2NCH_2^+$ ion, after loosing a terminal methyl group), while that for BP was instead 91 (corresponding to the benzyl moiety: $PhCH_2^+$). Thereby, in the TGA-MS experiments, the release of water as a function of the temperature was monitored by following the presence in the evolved gases of m/z = 18, while desorption of the organic TEA and BP was monitored by following the m/z values of 86 and 91, respectively. The inorganic composition of the samples was

characterized by elemental analysis (ICP-OES, Perkin Elmer Optima 3300 DV) and SEM/EDS (JEOL JSM-6400 Philips XL30 operating at 20 kV).

Solid state Nuclear Magnetic Resonance (NMR) spectra were recorded with a Bruker AV 400 WB spectrometer, using a BL7 probe for ^{29}Si and a BL4 probe for ^{31}P and ^{27}Al. ^{29}Si spectra were acquired using pulses of 3.3 μs to flip the magnetization 3 π/8 rad and a recycle delay of 240 s. For the acquisition of these ^{29}Si spectra, the samples were span at the magic angle (MAS) at a rate of 5–5.5 kHz. For ^{31}P, π/2 rad pulses of 4.25 μs and recycle delays of 80 s were used. The ^{27}Al spectra were measured using pulses of 1 μs to flip the magnetization π/12 rad, and delays of 1 s between two consecutives pulses. Both ^{31}P and ^{27}Al spectra were recorded while spinning the samples at ~11 kHz. All the NMR spectra were recorded for the calcined samples.

Infrared spectra of the calcined samples were recorded in the transmission mode using a Nicolet 5ZDX FTIR spectrometer provided with an MCT detector. Spectra in the 4000-1000 cm^{-1} range were acquired at 4 cm^{-1} resolution by averaging 250 scans and using Happ-Genzel apodization. The samples were pressed into thin self-supporting wafers (thickness, *ca.* 6 $mg \cdot cm^{-2}$) and introduced in an all-glass IR cell provided with CaF_2 windows. The sample wafers were pre-treated at 450 ºC for 1 hour under synthetic air flow and subsequently in a vacuum (10^{-3} Pa) at 350 ºC for 15 h. FTIR spectra were recorded at room temperature.

The catalytic activity of the samples was tested in the isomerisation of m-xylene reaction; m-xylene was purchased from Scharlau (99%). These experiments were carried out in a differential fixed-bed reactor operating with continuous feed and nitrogen as carrier gas at atmospheric pressure. All the samples were previously activated in air flow (100 ml/min) at 450 ºC for 1 hour. Then the flow was changed to N_2 and the temperature decreased to 350 ºC, keeping these conditions for 1 more hour,

after which the reaction was performed at the same temperature. In order to obtain conversions of about 10 %, contact times were varied, while the molar ratio was fixed at a N_2/m-xylene ratio of 5.29. The reaction products were analysed by gas chromatography using a 2 m x 3 mm OD packed column filled with 16% DC-200 methylsilicone and 3 % Bentone 34 on 80–100 mesh ChromosorbW. A Varian 3800 gas chromatograph provided with a flame ionisation detector (F.I.D.) was used in the analysis. Due to coke deposition, initial activities (v_0) at zero reaction time were calculated for each product [20].

Results

Synthesis Results

Hereafter, samples will be named making reference to the amount of TEA and BP used in the synthesis; in this way, (1.5T), (1T,0.5B), (0.5T,1B) and (1.5B) will refer to SAPO-5 materials obtained with 1.5 TEA, 1 TEA : 0.5 BP, 0.5 TEA : 1 BP and 1.5 BP SDA molar compositions, respectively.

XRD patterns (Figure 1) of the as made samples revealed that SAPO-5 was crystallized both with the pure SDAs and with the different combinations of SDAs, being the crystallinity of the samples very similar to each other, with that for SAPO-5 obtained with TEA as the only SDA reaching the highest value.

The incorporation of the organic (TEA and BP) and water molecules was studied by TGA (after the hydration treatment) (Figure 2). The TGA profiles show up to four different weight loss steps, whose magnitude and temperature range depend on the SDA used in the synthesis. A first step is found for all the samples at temperatures below 120 ºC, which is assigned to desorption of water. The lack of organic loss in this temperature range was confirmed by TGA-MS experiments (see below). At

temperatures above 120 ºC, several weight loss steps occur, which extend to temperatures as high as *ca.* 700 ºC, evidencing the removal of organic molecules occluded within the AFI channels. The sample containing only TEA as SDA (1.5T) shows two main weight losses in this temperature interval. Removal of TEA seems to occur mainly at temperatures around 400 ºC, although some remaining chemical species derived from TEA combustion in air are desorbed at higher temperatures (around 600 ºC). In contrast, the sample synthesised using only BP as SDA (1.5B) shows the most intense weight loss at *ca.* 600 ºC. Nevertheless, an additional weight loss is observed at temperatures around 200 ºC that probably comes from the desorption of uncharged BP possibly occluded associated to Si islands. Finally, for the samples synthesised using different combinations of both SDAs, three weight loss steps at around 200, 400 and 600 ºC are observed, suggesting that the samples contain both organic compounds.

TGA (in helium) coupled to mass spectrometry experiments were performed aiming to verify the incorporation of the two SDA molecules within the AFI structures (Figure 3). The MS spectra of the evolving gases evidence that, at temperatures below 120 ºC, only water is desorbed. MS spectra of the samples obtained with one single SDA evidence that desorption of BP under helium can be characterised by the evolution of a fragment with an m/z value of 91 at temperatures around 400 ºC. The fact that no peak at 200 ºC is observed here could be due to desorption of weakly retained, uncharged BP during the stabilisation time of the MS. Desorption of TEA gives rise to a signal at m/z = 86 in the temperature range from 150 to 450 ºC, with only a minor contribution to the signal at m/z = 91 at temperatures around 400ºC. The comparison of these data with the MS profiles obtained for the samples synthesised using simultaneously both SDAs confirm that these later samples contain both SDAs occluded.

In order to determine the organic content of the samples, CHN elemental analyses were also carried out (Table 1). The C/N ratios of the samples obtained with only one type of SDA [(1.5T) and (1.5B)] were very similar to those of the free molecules, evidencing the resistance of the molecules to the hydrothermal treatment and their integral incorporation within the AFI structure. Indeed, the values for the samples where a mixture of SDAs was used were also similar to those expected for a mixture of the two molecules in the same molar ratio as in the synthesis gel. These results provide evidence about the incorporation of the SDAs in a similar ratio as in the synthesis gel, and highlight the absence of a preferred incorporation of one type of SDA, and thus the absence of a competitive structure directing effect between the two types of molecules. The total organic contents of the SAPO-5 materials (Table 1) were calculated from the amount of carbon determined by elemental analysis results and assuming that the SDA molecules were incorporated in the same ratio as they were in the synthesis gels. The results evidence an increase of the organic content in the samples, on a weight bases, with the molar fraction of BP in the synthesis gel. However, the N content (Table 1) was nearly the same in all the materials, which indicates that the total number of SDA molecules per unit cell did not vary with the use of the different SDA combinations (the N content can be taken as an estimation of the number of molecules in the solids since both TEA and BP have one N atom per molecule). For all samples, the estimated total concentration of SDAs is in the range 1.3–1.4 molecules per unit cell (estimated as organic content referred to final weight determined by TGA).

Table 1 also shows the estimated water content of the as-synthesised samples. Most of the adsorbed water was desorbed at temperatures below 120 ºC in the TGA experiments. However, the water content could not be directly measured from TGA since water release is in some points overlapped with organic desorption (see Figure 3).

In order to obtain more accurate results, the water content was calculated as the difference between the total weight loss measured by TGA and the estimated weight of organic compounds. These amounts were also corrected by the weight loss due to removal of hydroxyl groups (around 1 wt%). The amount of hydroxyl groups present in the materials was calculated from the TGA of the calcined samples, by measuring the weight loss observed at temperatures above 200 ºC, where the water desorption has already ended.

The differences in the organic and water contents in the samples (normalising the values given in Table 1 to the inorganic content of each sample) as a function of the BP (or TEA) content are shown in Figure 4 (in weight % per 100 g of calcined AFI material). It can be clearly observed that the total organic content increases when the content in BP increases, or in other words, when the TEA content decreases. In addition, the water content follows the opposite trend: it decreases when the BP content increases (and vice versa for TEA) which is probably due to the lower occlusion of TEA in the channels, promoting a higher water occlusion in order to completely fill the void space left by the occlusion of TEA. This means that the BP SDA fills more efficiently the AFI channels than TEA.

Crystal size and morphology were studied by SEM (Figure 5), which revealed a similar crystal pattern for all the samples: all the SAPO-5 materials crystallized as spherical aggregates of small and planar crystals.

The inorganic composition of the SAPO-5 samples (Si, Al and P contents) was measured by SEM/EDS and ICP-OES (Table 2). The corresponding atomic ratios Al:Si+P are 0.54:0.46. The Si content measured by ICP-OES is 9 wt.% for sample (0.5T,1B), in agreement with the content determined by SEM/EDS. For the rest of the samples, the values obtained by ICP-OES are slightly higher (ca. 11 wt%). This

difference could be due to the fact that SEM/EDS measures the composition of the SAPO-5 crystals (and only reaches the crystal surface), while ICP-OES gives an average of the Si content in the overall sample (including possible amorphous material accompanying the SAPO-5 structure). SEM/EDS analyses show a high homogeneity of the Si content in each sample, which corresponds to 3.5-4.5 Si atoms per unit cell. Both techniques suggest that the Si content of the different SAPO-5 materials is very similar, and thus that the use of the different SDA combinations does not lead to a different total incorporation of Si (although it can lead to different incorporation mechanisms, as we will see below).

The incorporation of the inorganic atoms in the SAPO-5 structure was studied also by Solid State MAS NMR. ^{31}P NMR spectra of the calcined samples (Figure 6-left) show small differences among the SAPO-5 materials: a main signal is observed at –31 ppm, which is typical of P atoms in a tetrahedral environment in the AFI structure [21]. In addition, a small shoulder in the –15 to –20 ppm range is observed for all the samples, although its intensity is lower for the SAPO-5 material obtained with TEA as the only SDA. This resonance is usually assigned to defect sites of O_3PO^- or O_3POH types, probably related to terminal defects or to the presence of minor quantities of some amorphous material accompanying the SAPO-5 structure [21]. This resonance shows a lower intensity for sample (1.5T), suggesting a higher crystallinity of this sample, in agreement with the XRD results. ^{27}Al NMR spectra of the calcined samples (Figure 6-right) show in all the samples three peaks centred at 38, 8 and –11 ppm, corresponding to the presence of Al in tetrahedral, pentacoordinated and octahedral environments within the AFI structure, respectively [21,22]. The only difference among the materials is observed in the resonance corresponding to pentacoordinated Al atoms, which increases as the BP content in the synthesis gel increases.

Finally, the incorporation of Si in the SAPO-5 structures through the different mechanisms was studied by ^{29}Si MAS NMR (Figure 7). As stated in the introduction, different Si environments can be present in SAPO-5 materials depending on the substitution mechanisms whereby Si is incorporated in the AFI structure. $Si(OAl)_4$ environments, coming from the occurrence of solely the SM2, gives a signal centred at around –90 ppm, while $Si(OSi)_4$, coming from the presence of Si islands formed through the combined SM2+SM3 mechanism, gives a resonance at lower shifts, centred at around –112 ppm [23]; $Si(OAl)_3(OSi)$, $Si(OAl)_2(OSi)_2$ and $Si(OAl)(OSi)_3$ environments, that are located at the borders of the Si islands, give place to signals within this range, shifted towards higher fields as the number of surrounding Si atoms in the second coordination shell increases. Therefore, ^{29}Si NMR is able to quantitatively determine the extent of each SM whereby Si is incorporated in the microporous structure, and so the concentration and size of the resulting Si islands. The spectra of the calcined SAPO-5 samples (Figure 7) showed a higher presence of $Si(OAl)_4$ in the sample obtained with TEA as the only SDA; in addition, the signal for Si islands is shifted towards higher fields (with respect to the Si island signal of the other samples), suggesting a smaller size of the islands. The incorporation of BP in the synthesis gels brings a reduction of the $Si(OAl)_4$ band and a simultaneous increase of the intensity of the one associated to Si in islands, which is also shifted towards higher fields as the relative amount of BP increases, suggesting a larger size of the Si islands for samples obtained with BP. These results clearly evidence a higher trend of Si to be incorporated through the SM2 when TEA is the SDA, leading to isolated $Si(OAl)_4$ environments, or through the SM2+SM3 when BP is used, resulting in a major formation of Si islands. Interestingly, it seems that the ratio at which these opposite trends occur can be tailored to a certain point by the ratio of each SDA used in the synthesis gel.

Acidity and Catalytic Activity Results

The effect of SDAs on the concentration of the acidic (bridging) hydroxyl groups in the calcined SAPO-5 materials has been studied by FTIR spectroscopy. The spectra show up to 5 distinct bands in the O-H stretching region (Figure 8). All the spectra exhibit the two bands characteristic of acidic, bridging hydroxyl groups (Si-OH-Al) in SAPO-5, centred at 3626 and 3512 cm^{-1} [24-27], assigned to isolated OH species located in the large 12-membered rings and OH species interacting with framework oxygen atoms in the 6-member rings, respectively [24]. Furthermore, two bands appear at 3678 and 3744 cm^{-1}, corresponding to terminal P-OH and Si-OH groups, respectively [24-27]. Finally, an additional very weak band appear in the spectra of sample 1.5B at *ca.* 3790 cm^{-1}, which can be attributed to terminal Al-OH groups.

As shown in Figure 8, the terminal Si-OH and P-OH bands in the normalized spectra are of similar intensity for all samples, in agreement with the similar crystal sizes observed by SEM. However, relatively large differences in intensity can be observed for the two bridging hydroxyl bands among the four spectra. The highest intensity corresponds to sample 1.5T, for which the areas of both bands are more than 3 times higher than those of sample 1.5B, the one with the less intense bands. For the two samples synthesized using a combination of TEA and BP, these bands show similar intensity (although they seem slightly lower for sample (1T,0.5B)), in between those of 1.5B and 1.5T. These results evidence a marked effect of the SDA molecule on the concentration of Brønsted sites, associated to Si-OH-Al groups. Taking into account that all samples possess similar Si contents (see above), the differences in acid sites concentration observed by FTIR indicates a strong variation of the average H^+ / Si ratio, and can be therefore interpreted as a result of a different Si distribution, in agreement

with the ^{29}Si NMR data. The sample synthesized using only TEA as SDA, which exhibits the largest concentration of bridging hydroxyls, would possess the highest concentration of $Si(OAl)_4$ and the smallest Si islands. Partial replacement of TEA by BP seems to produce larger Si islands, as indicated by the lower acid sites content. This tendency of BP to increase the size of silicon islands is also observed for the sample obtained with pure BP, which exhibits the lowest concentration of Si-OH-Al species.

Finally, the catalytic activity of these materials was studied in a test reaction typically employed for characterization of microporous materials, the isomerisation of m-xylene. Apart from the isomerisation of m-xylene to give the ortho- and para-xylene isomers, disproportionation can also take place, resulting in toluene and trimethylbenzene products; the reaction rate for each of these reactions are shown in Table 3. The results clearly demonstrate that the total reaction rate (isomerisation and disproportionation) gradually increases with the BP content in the synthesis gels up to 1 mol of BP, remaining practically unchanged for 1.5 mol of BP. If we now look at the partial reaction rates (Table 3), it is interesting to note the difference in the two reaction rates between samples (0.5B,1T) and (1.5B), where the isomerisation reaction slightly decreases with an increase of the BP content while the disproportionation reaction increases. These results seem to indicate that there is an optimum TEA/BP content for the isomerisation reaction, corresponding to sample (0.5T,1B), what brings the existence of an optimum size and concentration of the Si islands for the catalysis of the isomerisation reaction, achieved by this TEA/BP ratio (0.5T,1B). In this case, the acid sites are strong enough to efficiently catalyse the isomerisation reaction; however, a further reduction of the TEA content and increase of BP implies a higher acid strength but also a lower concentration of Brønsted sites, resulting in a slight decrease of the isomerisation reaction rate. Instead, the disproportionation reaction rate increases also

from sample (0.5T,1B) to (1.5B), evidencing a higher acid strength required for this catalytic reaction, as suggested earlier [20]. These observations suggest the existence of different optimum Si island sizes for the catalysis of the isomerisation or disproportionation reactions.

Discussion

Our results evidence that the use of different SDAs in the synthesis of SAPO-5 catalysts leads to differences in the catalytic activity of the obtained materials. We have found that BP as SDA leads to an improved catalytic activity compared to TEA. Since the total incorporation of Si and the crystal size and morphology are similar in all the materials, such an improvement must be due to a different mechanism in the incorporation of Si in the AlPO network: BP drives the incorporation of Si towards the formation of large Si islands, whose Brønsted sites usually have a higher acid strength, while the SM2 incorporation of Si, giving isolated $Si(OAl)_4$ environments, is more favored when TEA is used as the SDA, leading to an increase in the number of Brønsted acid sites, as shown by FTIR, but of lower strength. It also seems that the use of BP brings a higher penta-coordination of Al in the calcined samples, and thus it seems to be associated to the presence of large Si islands, although so far the reason for this is not clear.

The results from the organic content determination evidence that, despite the different molecular size, both molecules are incorporated within the AFI structure in a similar amount (in terms of number of molecules per unit cell, i. e. packing value, around 1.3 to 1.4 TEA and/or BP molecules per unit cell). This similarity indicates that the difference observed in the mechanism of Si incorporation cannot be only due to a different packing value of the molecules, and thus to a different amount of positive charges available to

charge-balance the negative charge generated by the incorporation of Si through SM2, as stated by Barthomeuf and coworkers in the synthesis of SAPO-34 with morpholine or tetraethylammonium hydroxide [17]. The packing values we have found involve a different organic content (in wt %) due to the different molecular weight of both molecules (102 and 162 for protonated TEA and BP, respectively), showing a higher filling efficiency of BP. In order to completely fill the void space of the microporous structure left by the organic SDAs, and thus provide further stabilization to the system during crystallization, water is incorporated within the structure, not only in the 6 MR channels but also in between the organic molecules [19]. Thereby, the lower organic content of the SAPO-5 materials obtained with TEA involves a higher water occlusion (and the opposite for BP), resulting in a higher hydrophilicity in the channels of the AFI structure obtained with TEA. Such difference in hydrophilicity could be the reason for the different mechanism of Si incorporation observed in the materials when using TEA or BP as SDAs. SM2 gives $Si(OAl)_4$ environments (and thus a negative charge per Si in the lattice), which are more hydrophilic than the Si islands formed through the SM2+SM3 mechanism, where the silica-type domain increases the hydrophobicity of the lattice.

The catalytic activity results indicate that the samples obtained with BP as the main SDA are more active than those where TEA is the major SDA, despite the higher abundance of Brønsted acid sites of the latter, as shown by FTIR. This evidences that the m-xylene isomerisation reaction is more efficiently catalysed by Brønsted acid sites associated to large Si islands, whose acid strength is higher, than with isolated Si Brønsted acid sites (in $Si(OAl)_4$ environments).

Interestingly, it has been found that the catalytic activity, and thus the Si incorporation mechanism, follows a direct relation with the TEA/BP ratio in the mixture of SDAs

employed in the synthesis, suggesting that the effects of both SDAs over the substitution mechanisms of Si are additive. This means that we could tailor, at least to a certain point, the mechanisms by which Si is incorporated in AlPO networks, by using combinations of these two SDAs. In last term, our methodology could provide an easy control of the acid strength of SAPO materials by just varying the relative ratio of the two SDAs. This issue is very important in catalysis, since different reactions usually require different acid strengths in order to get the desired products under the best operative conditions.

Conclusions

In this work we have demonstrated that different organic molecules employed in the synthesis of SAPO-5 catalysts can lead to different Si distributions within the $AlPO_4$ lattices; this concept could lead to a rational choice of the organic molecules that will be used for structure-directing the synthesis of the desired SAPO catalyst.

We have found that TEA molecules lead to an incorporation of Si mainly as isolated Si atoms through the SM2 mechanism, giving place to more hydrophilic structures, while BP drives the incorporation towards the formation of large Si islands, increasing the hydrophobicity of the material. This difference can be explained in terms of the different hydrophilic/hydrophobic character that the use of both molecules as SDAs imprints in the solids. TEA incorporation within the AFI structure is lower than BP one on a weight bases, and thus brings the simultaneous incorporation of water in order to fulfil the void spaces of the microporous structure to make the crystallization energetically viable, thus providing a more hydrophilic nature to the AFI channels. Instead, incorporation of BP carries a lower water incorporation, therefore yielding a more hydrophobic network. It has been found that Brønsted acid sites associated to the

large Si islands provided by the use of BP are much more active in the isomerisation of m-xylene than those related to $Si(OAl)_4$ environments produced by the use of TEA.

Interestingly, we have observed that the change in catalytic activity properties provided by the use of the two SDAs is gradual; mixtures of SDAs yield SAPO-5 materials with Si distributions related to the relative ratio of TEA/BP SDAs used in the synthesis gels. Therefore, this concept could provide a very useful and efficient methodology to tailor the Si substitution mechanisms by which it is incorporated in SAPO-5 materials, thereby controlling their acid strength, through the rational choice of the kind and ratio of SDAs used in the synthesis. This methodology could in principle be extended to other SAPO materials with different structures.

ACKNOWLEDGMENT.

Financial support of the Spanish Ministry of Education and Science (project CTQ2006-06282) is acknowledged. LGH acknowledges the Spanish Ministry of Education and Science for a postdoctoral grant. T. Blasco is acknowledged for collecting the NMR spectra, and E. Sastre for his help with the TGA-MS experiments.

Table 1. Elemental analyses of the different samples, and calculated organic and water contents, as calculated from EA and TGA data.

	Gel composition		Elemental analysis				Calculated content in the samples			
	Molar		wt. %		C/N		wt. %		Molecules per u.c.	
Sample	TEA	BP	C	N	Exp.	Theor. [a]	Organic	H_2O	SDA	H_2O
(1.5T)	1.5	0.0	5.45	1.14	5.6	6.0	7.7	5.6	1.3	5.3
(1T,0.5B)	1.0	0.5	7.57	1.18	7.5	7.7	10.0	5.1	1.4	5.0
(0.5T,1B)	0.5	1.0	8.47	1.14	8.7	9.3	10.8	3.7	1.4	3.5
(1.5B)	0.0	1.5	9.41	1.10	10.0	11.0	11.6	3.9	1.3	3.8

[a] C/N ratio expected for samples containing the two SDAs compounds in the same molar ratio as used in the synthesis gel.

Table 2. Chemical composition (wt. %) of the SAPO-5 samples, as measured by SEM/EDS and ICP-OES.

	SEM/EDS			ICP-OES		
Sample	**Al**	**Si**	**P**	**Al**	**Si**	**P**
(1.5T)	50.2	8.7	41.1	42.6	11.1	46.3
(1T,0.5B)	50.7	7.0	42.4	42.5	10.8	46.7
(0.5T,1B)	50.6	9.4	40.1	43.1	9.0	48.0
(1.5B)	50.5	8.6	40.9	42.8	10.6	46.6

Table 3. Total, isomerisation and disproportionation initial reaction rates (r_0) for the different samples. The rates are given in $mol \cdot h^{-1} \cdot g^{-1}$.

Sample	**Total r_0**	**Isom r_0**	**Disp r_0**
(1.5T)	0.208	0.133	0.075
(1T,0.5B)	0.355	0.275	0.081
(0.5T,1B)	0.477	0.367	0.110
(1.5B)	0.485	0.321	0.164

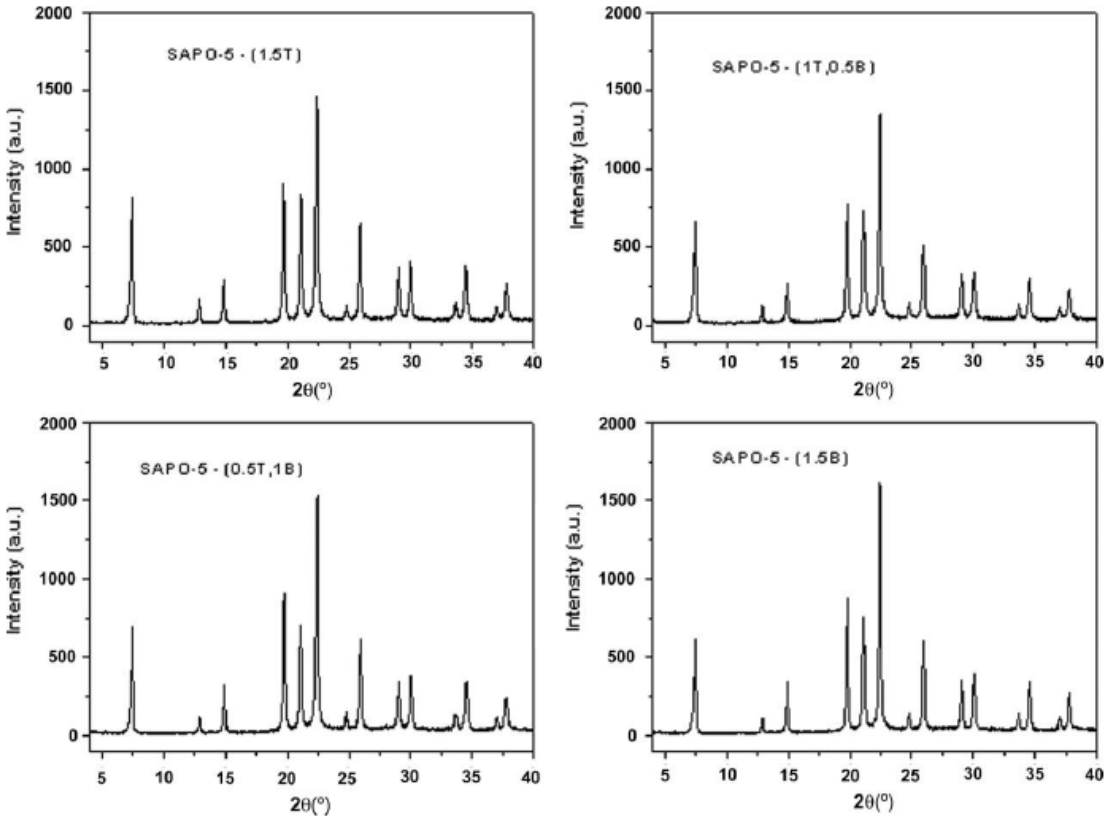

Figure 1. XRD patterns of the SAPO-5 samples.

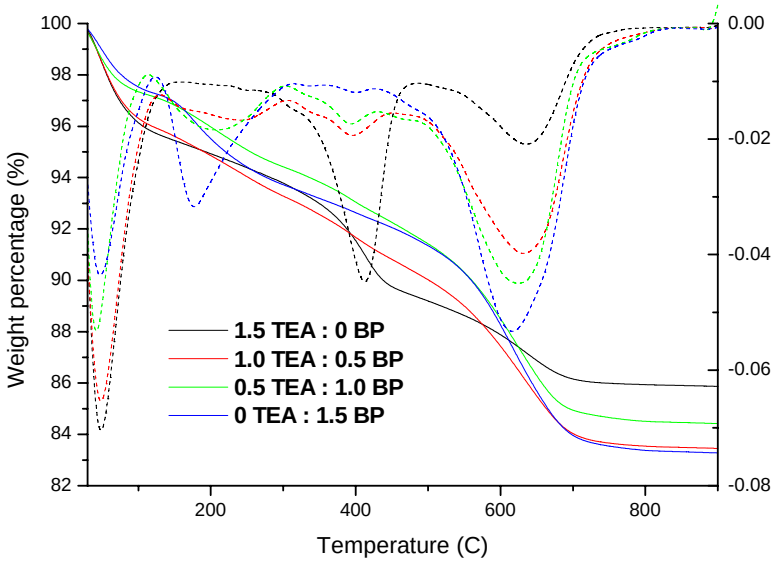

Figure 2. TGA (solid lines) and DTA (dashed lines) of the SAPO-5 samples.

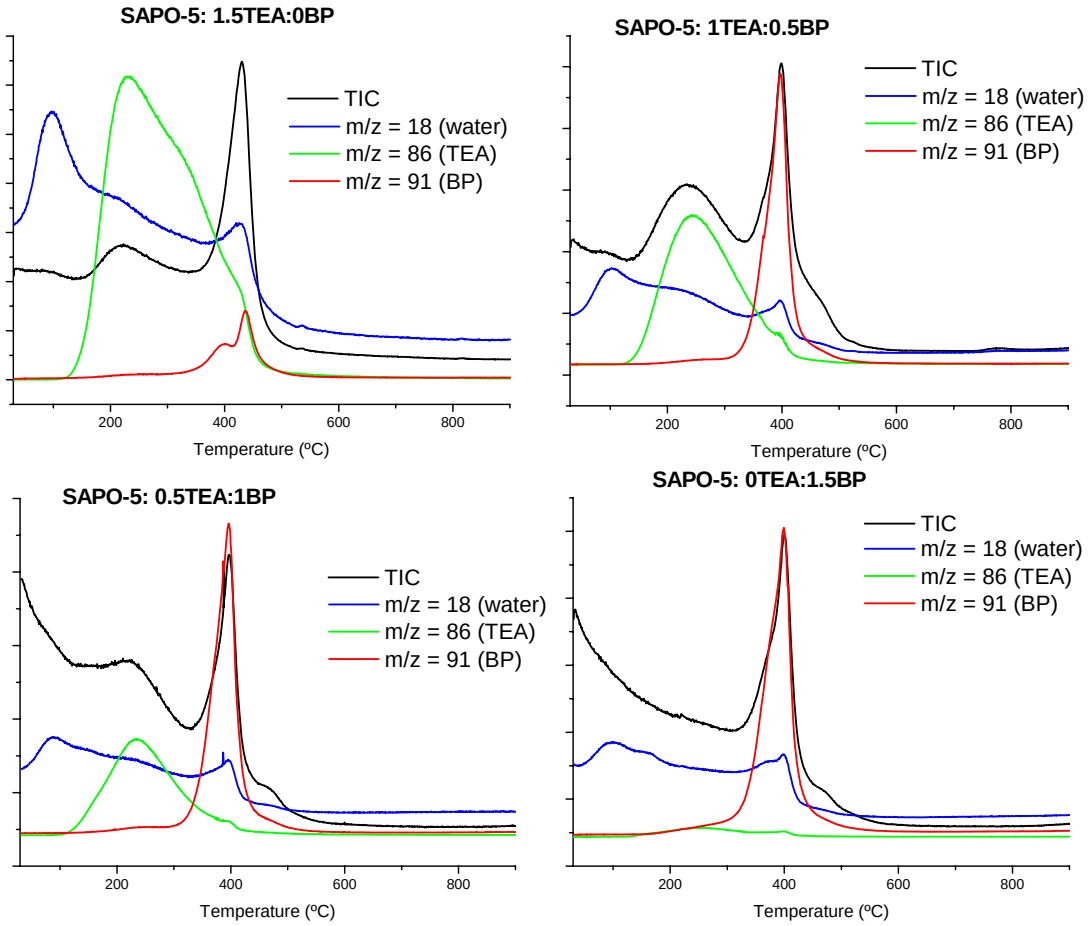

Figure 3. TG-MS experiments of the different SAPO-5 samples. Desorption of the different species was monitored by following the m/z values of 18 (for water), 86 (for TEA) and 91 (for BP). Counts for m/z of 18, 86 and 91 are plotted under the same scale, while total ion counts (black line, referred as TIC) is plotted in a different scale.

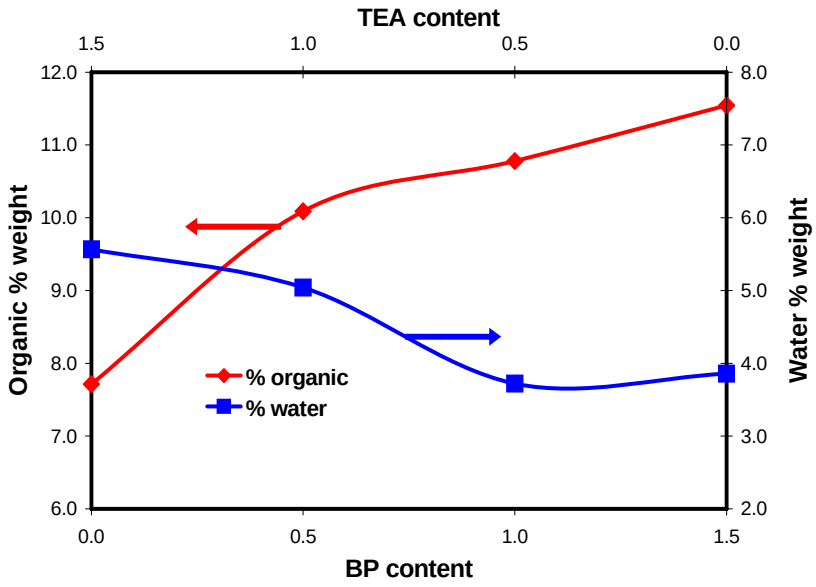

Figure 4. Organic (black, left axis) and water (grey, right axis) contents (normalised to the inorganic content of the samples remaining at the end of the TGA analyses) in the different SAPO-5 materials as a function of the SDAs employed in the synthesis. The values are expressed as weight per 100 g of calcined AFI material.

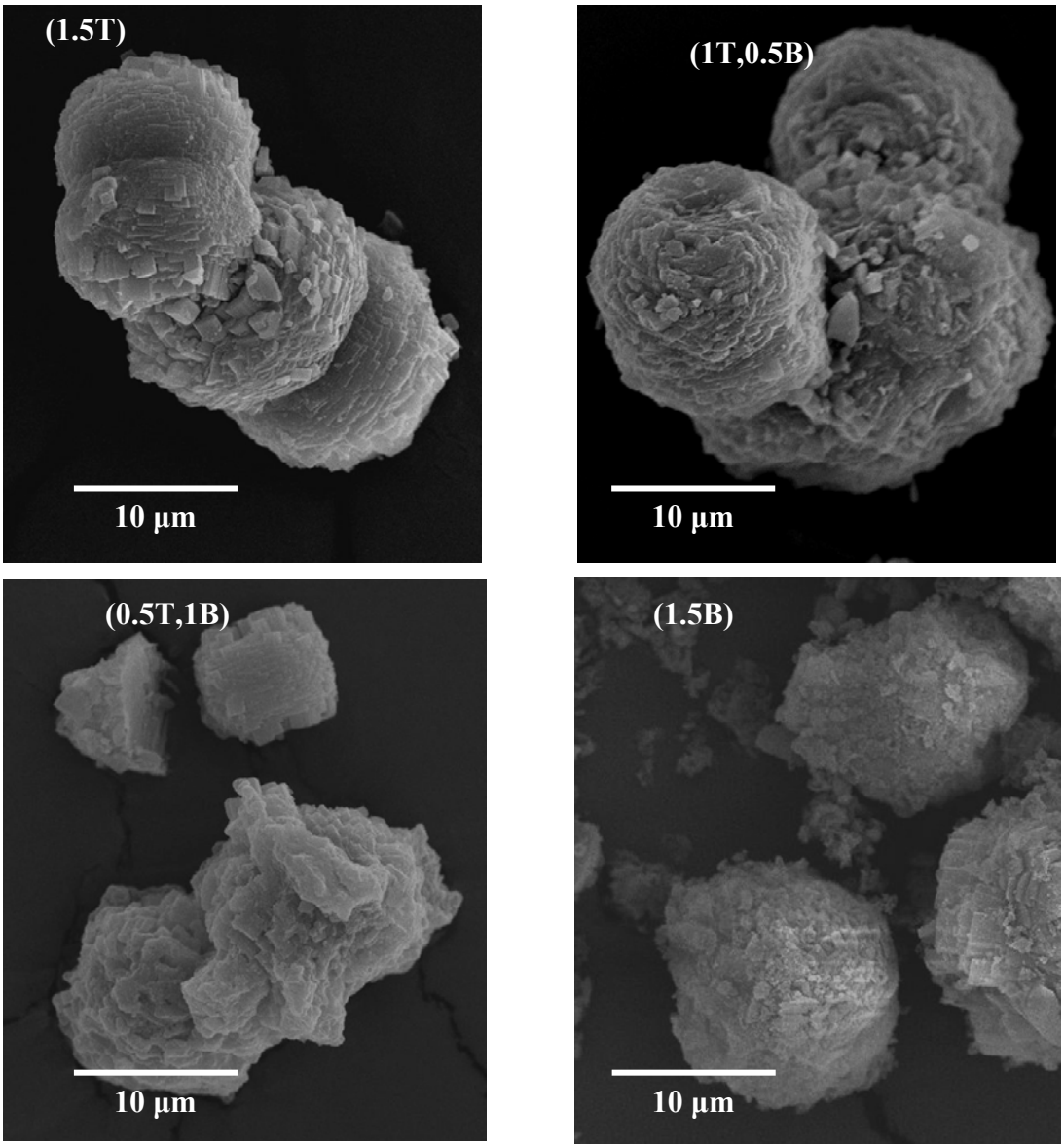

Figure 5. SEM pictures of SAPO-5 samples (x2500 magnification).

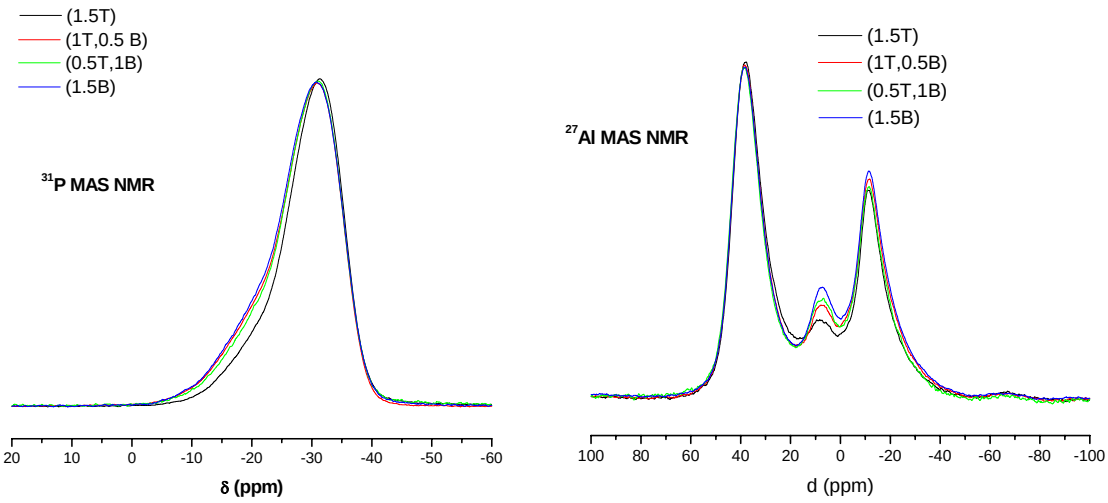

Figure 6. ^{31}P NMR (left) and ^{27}Al NMR (right) spectra of the different SAPO-5 samples after calcination.

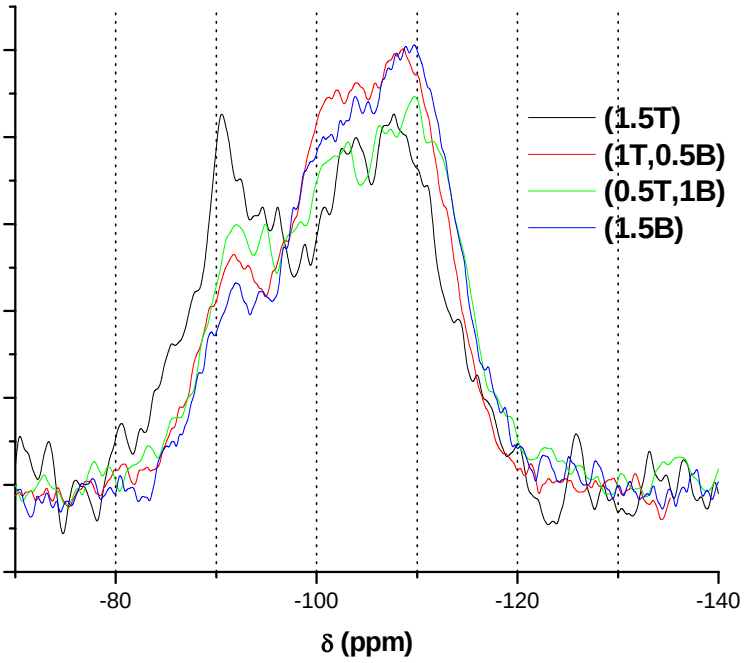

Figure 7. ^{29}Si NMR of the different SAPO-5 samples after calcination. The spectra have been normalised to the same total area.

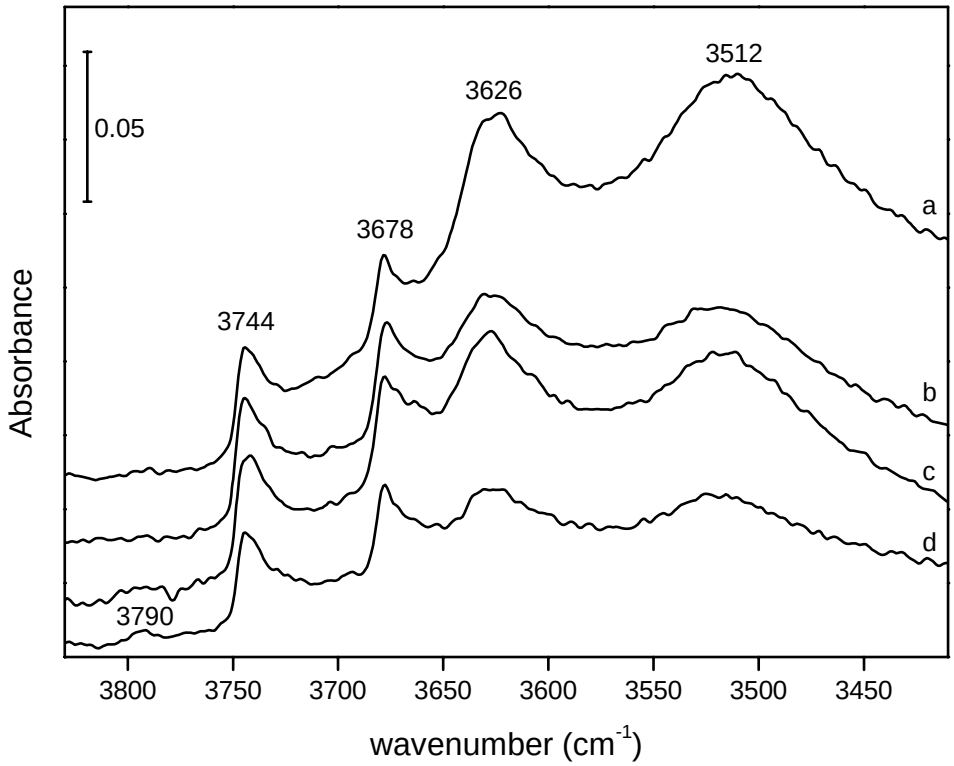

Figure 8. Normalized FTIR spectra of calcined samples (1.5T) (a), (1T,0.5B) (b), (0.5T,1B) (c) and (1.5B) (d).

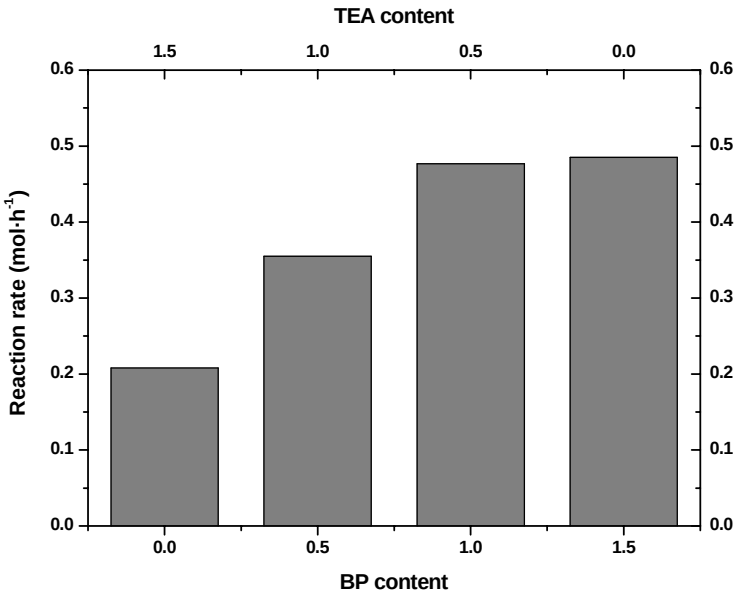

Figure 9. Reaction rate for the m-xylene isomerization as a function of the SDAs employed in the synthesis.

References

[1] S. T. Wilson, B. M. Lok, E. M. Flanigen, E. M. US Patent, 4310440, 1982.

[2] http://www.iza-structure.org/databases

[3] T. Masukawa, T. Komatsu, T. Yashima, Zeolites 18 (1997) 10.

[4] M. Montoya-Urbina, D. Cardoso, J. Pérez-Pariente, E. Sastre, T. Blasco, V. Fornés, J. Catal. 173 (1998) 501.

[5] A. K. Sinha, S. Sainkar, S. Sivasanker, Microporous Mesoporous Mater. 31 (1999) 321.

[6] V. Hulea, N. Bilba, M. Lupascu, E. Dumitriu, D. Nibou, S. Lebaili, H. Kessler, Microporous Mater. 8 (1997) 201.

[7] M. Hochtl, A. Jentys, H. Vinek, Appl. Catal. A: General 207 (2001) 397.

[8] U. Sridevi, V. V. Bokade, C. V. V. Satyanarayana, B. S. Rao, N. C. Pradhan, B. K. B. Rao, J. Mol. Catal. A: Chem. 181 (2002) 257.

[9] J. Chen, P. A. Wright, S. Natarajan, J. M. Thomas, in: J. Weitkamp, H. G. Karge, H. Pfeifer, W. Hölderich (Eds.), Zeolites and Related Microporous Materials: State of the Art, Stud. Surf. Sci. Catal. 84 (1994) 1731.

[10] J. A. Rabo, R. J. Pellet, P. K. Coughlin, E. S. Samshoum, in: H. G. Karge, J. Weitkamp (Eds.), Zeolites as Catalyts, Sorbents and Detergent Builders, Stud. Surf. Sci. Catal. 46 (1989) 1.

[11] L. Sierra de Saldarriaga, C. Saldarriaga, M. E. Davis, J. Am. Chem. Soc. 109 (1987) 2686.

[12] D. Hasha, L. Sierra de Saldarriaga, C. Saldarriaga, P. E. Hathawya, D. F. Cox, M. E. Davis, J. Am. Chem. Soc. 110 (1988) 2127.

[13] D. Barthomeuf, Zeolites 14 (1994) 394.

[14] L. Wang, C. Guo, S. Yan, X. Huang, Q. Li, Microporous Mesoporous Mater. 64 (2003) 63.

[15] S. Seelan, A. K. Sinha, J. Mol. Catal. A: Chem. 215 (2004) 149.

[16] H. Gies, B. Marler, Zeolites 12 (1992) 42.

[17] R. Vomscheid, M. Briend, M. J. Peltre, P. P. Man, D. Barthomeuf, J. Phys. Chem. 98 (1994) 9614.

[18] P. Liu, J. Ren, Y. Sun, Microporous Mesoporous Mater. 114 (2008) 365.

[19] L. Gómez-Hortigüela, J. Pérez-Pariente, F. Corà, Chem. Eur. J., published in web. DOI : 10.1002/chem.200801458.

[20] J. A. Martens, J. Pérez-Pariente, E. Sastre, A. Corma, P. A. Jacobs, Appl. Catal. 45 (1988) 85.

[21] L. Gómez-Hortigüela, J. Pérez-Pariente, T. Blasco, Microporous Mesoporous Mater. 78 (2005) 189.

[22] R. Jelinek, B. F. Chmelka, Y. Wu, M. E. Davis, J. G. Ulan, R. Gronsky, A. Pines, Catal. Lett. 15 (1992) 65.

[23] C. S. Blackwell, R. L. Patton, J. Phys. Chem. 92 (1988) 3965.

[24] K.-H. Schnabel, G. Finger, J. Kornatowski, E. Löffler, C. Peuker, W. Pilz, Microporous Mater. 11 (1997) 293.

[25] G. Lischke, B. Parlitz, U. Lohse, E. Schreier, R. Fricke, Appl. Catal. A 166 (1998) 351.

[26] G. Müller, J. Bódis, G. Eder-Mirth, J. Kornatowski, J. A. Lercher, J. Mol. Struct. 410-411 (1997) 173.

[27] S. G. Hedge, P. Ratnasamy, L. M. Kustov, V. B. Kazansky, Zeolites 8 (1988) 137.